



A Journal of the Gesellschaft Deutscher Chemiker

# Angewandte Chemie

GDCh

International Edition

[www.angewandte.org](http://www.angewandte.org)

## Accepted Article

**Title:** Photochemical Electrocyclization of Poly(phenylacetylene)s:  
Unwinding Helices to Elucidate their 3D-Structure in Solution

**Authors:** Felix Freire, Emilio Quiñoá, Ricardo Riguera, Rafael Rodríguez, and Francisco Rey-Tarrío

This manuscript has been accepted after peer review and appears as an Accepted Article online prior to editing, proofing, and formal publication of the final Version of Record (VoR). This work is currently citable by using the Digital Object Identifier (DOI) given below. The VoR will be published online in Early View as soon as possible and may be different to this Accepted Article as a result of editing. Readers should obtain the VoR from the journal website shown below when it is published to ensure accuracy of information. The authors are responsible for the content of this Accepted Article.

**To be cited as:** *Angew. Chem. Int. Ed.* 10.1002/anie.202014780

**Link to VoR:** <https://doi.org/10.1002/anie.202014780>

## RESEARCH ARTICLE

# Photochemical Electrocyclization of Poly(phenylacetylene)s: Unwinding Helices to Elucidate their 3D-Structure in Solution

Francisco Rey-Tarrío, Rafael Rodríguez, Emilio Quiñoá, Ricardo Riguera and Félix Freire\*

Francisco Rey-Tarrío, Dr. Rafael Rodríguez, Prof. Dr. Emilio Quiñoá, Prof. Dr. Ricardo Riguera, Prof. Dr. Félix Freire  
Centro Singular de Investigación en Química Biolóxica e Materiais Moleculares (CiQUS) and Departamento de Química Orgánica  
Universidade de Santiago de Compostela, E-15782 Santiago de Compostela, Spain

E-mail: felix.freire@usc.es

Supporting information for this article is given via a link at the end of the document

**Abstract:** Photochemical electrocyclization of poly(phenylacetylene)s (PPAs) is presented as a new tool for the structural elucidation of a polyene backbone, where important structural information such as  $w_1$  can be obtained. This new methodology allows not only the classification of PPAs in *cis-cisoidal* ( $w_1 < 90^\circ$ ) or *cis-transoidal* structures ( $w_1 > 90^\circ$ ), but also to obtain the approximate value of  $w_1$ , a crucial helical parameter. The process involves the irradiating a dilute PPA solution with visible light and monitoring the photochemical electrocyclization of the PPA helix by measuring the ECD spectra at different times. Thus, PPAs with a *cis-cisoidal* structure show a reduction of the ECD signal of at least 50% before 30 min of irradiation, while *cis-transoidal* helices need much longer time because the *transoidal* bond must be isomerized to *cisoidal* before the photochemical electrocyclization of the helix takes place. Moreover, the different *cis-cisoidal* and *cis-transoidal* helices require different times to decrease their ECD signal by 50% ( $t_{1/2}$ ), depending on the degree of compression or stretching of the helix, a fact that allows establishing a relationship between the secondary structure adopted by the PPA ( $w_1$ ) and the time required to lose the ECD vinylic signal by light irradiation. This process also permits the detection and identification of different helical scaffolds that can coexist in some solutions of the polymers.

## Introduction

The helix is a structural motif responsible of the function of biomolecules such as peptides, proteins, polysaccharides or DNA. This structure-function relationship has prompted the scientific community to study other non-natural helical materials such as helical polymers.<sup>[1-6]</sup> The importance of these materials lies in their wide applications in fields such as sensing,<sup>[7-15]</sup> asymmetric synthesis,<sup>[15-17]</sup> chiral recognition<sup>[18]</sup> and separation.<sup>[19-22]</sup> Among helical polymers, poly(phenylacetylene)s constitute a very interesting family due to their dynamic structure<sup>[23,25]</sup> where the flexibility of the polyenic backbone allows to tune the elongation<sup>[26-32]</sup> and the helical sense<sup>[33-43]</sup> of the polymer. These changes are triggered when an external stimulus interacts with the substituents modifying their steric and/or supramolecular interactions.<sup>[27-33,44]</sup> In such a way that the backbone prefers to adopt a different helix by changing the dihedral angle between conjugated double bonds. The skeleton of Poly(phenylacetylene)s (PPAs) can adopt four possible configurations, *cis-cisoidal*, *cis-transoidal*, *trans-cisoidal* and *trans-transoidal*, depending on the *cis/trans* structure of the double bond and the *cisoidal/transoidal* conformation around the

dihedral angle between conjugated double bonds [*cisoidal* ( $\omega_1 < 90^\circ$ ); *transoidal* ( $\omega_1 > 90^\circ$ )].<sup>[24]</sup>

Pleasantly, Rh(I) catalysts allows the formation of PPAs with *cis* configuration of double bonds.<sup>[45-47]</sup> A major problem emerges in the  $\omega_1$  dihedral angle control by monomer design,<sup>[48]</sup> where the balance between the steric and supramolecular interactions involved in the structure stabilization frequently allow for a single polymer to be constituted by an equilibrium mixture of several helices with different pitches and/or sense.<sup>[47-50]</sup>

Moreover, an important feature of PPAs is that the macromolecular helix is described by two coaxial helices. An internal helix determined by the conformation adopted by the polyene backbone, and the external one described by the pendant groups, which are arranged describing a helical structure, coaxial to the internal one. The *P/M* sense of the internal helix depends of the sign of the ( $\omega_1$ ) dihedral angle, that also influences the external helical direction. Thus, in *cis-cisoidal* helices ( $\omega_1 < 90^\circ$ ), the two helices rotate in the same sense [*P<sub>int</sub>*/*P<sub>ext</sub>* or *M<sub>int</sub>*/*M<sub>ext</sub>*], while in *cis-transoidal* ( $\omega_1 > 90^\circ$ ) polymers, both helices rotate in opposite directions [*P<sub>int</sub>*/*M<sub>ext</sub>* or *M<sub>int</sub>*/*P<sub>ext</sub>*].<sup>[51]</sup>

Hence, to build up the 3D-structure of a PPA, it is necessary to combine the information extracted by different techniques in solution and in the solid state —Nuclear Magnetic Resonance (NMR),<sup>[26,52-56]</sup> Differential Scanning Calorimetry (DSC),<sup>[56]</sup> Raman,<sup>[57]</sup> Raman Optical Activity (ROA),<sup>[58]</sup> Vibrational Circular Dichroism (VCD),<sup>[59]</sup> Electronic Circular Dichroism (ECD),<sup>[60-62]</sup> Atomic Force Microscopy (AFM),<sup>[50,64-72]</sup> X-Ray<sup>[73-82]</sup> as well as Time Dependent-Density Functional Theory (TD-DFT) calculations (Figure 1).<sup>[83-84]</sup> Nevertheless, a correct assignment of the *cis-cisoidal* (*c-c*) or *cis-transoidal* (*c-t*) configuration of the polyene backbone is far from solved because the DSC thermogram is affected by the pendant groups or even by the dynamic behavior of the polymer,<sup>[56]</sup> rendering the technique useless in many cases. Searching for a more robust technique to distinguish *cis-cisoidal* ( $\omega_1 < 90^\circ$ ) from *cis-transoidal* ( $\omega_1 > 90^\circ$ ) structures,<sup>[86-92]</sup> we turned our attention to some stimuli-triggered transformations that linked to the polymer structure, such as those produced by light, temperature or pressure. Thus, while high-pressure induces a *cis-to-trans* isomerization of double bonds by generation of radical species in the backbone, thermal treatment of poly(phenylacetylene) results in an intramolecular cyclization and subsequent chain cleavage of 1,3,5-triphenylbenzene derivatives. The reaction can be carried out in solution or in the solid state and stimulated with air, pressure or electric fields, but nevertheless, the reaction is not very effective and occurs partially.<sup>[86-94]</sup>

## RESEARCH ARTICLE

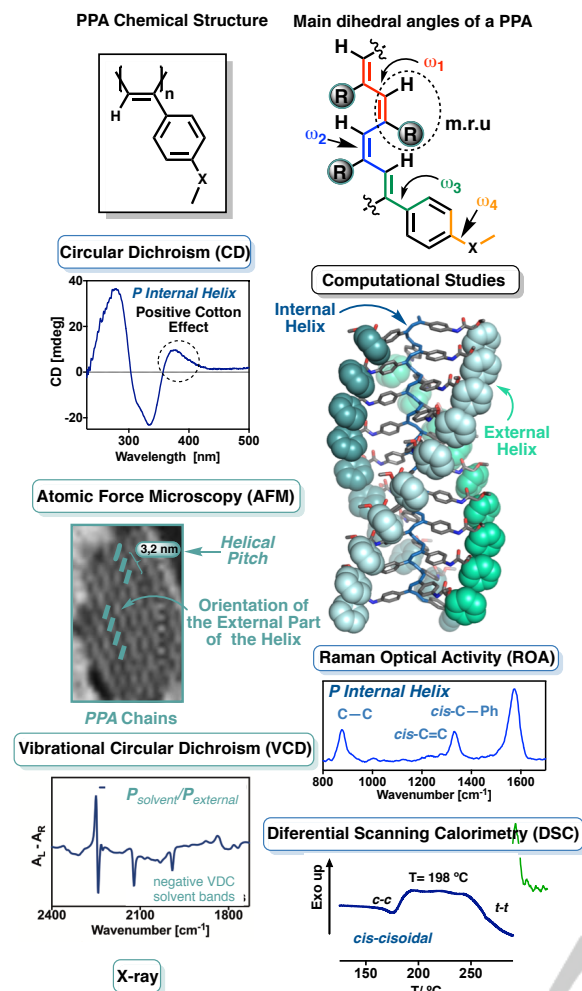


**Figure 1.** Chemical structure and main dihedral angles of PPAs. Combination of structural techniques—AFM, X-ray, DSC, computational studies, DFT, ECD, VCD, ROA—used to elucidate the 3D structures in PPAs.

In contrast, the controlled irradiation of PPAs under visible light leads to 1,3,5-triphenyl substituted benzenes in a highly selective intramolecular process.<sup>[56]</sup> From literature it is known that this photocyclic aromatization process takes place in the solid state, while in solution the reaction proceeds in small yields.<sup>[56]</sup> Interestingly, the reactivity of the polymer backbone depends directly on the configuration of the starting polyene—only those *cis-cisoidal* scaffolds with a short distance between double bonds ( $< 4\text{Å}$ ) were found to react—and it was used for the formation of self-supporting supramolecular polymeric membranes.<sup>[95,96]</sup> Herein, we will show that visible light photochemistry can be implemented as a unique structural tool to identify in solution not only the presence of a *cis-cisoidal* or *cis-transoidal* skeleton of a PPA, but also to provide an approximated dihedral angle for  $\omega_1$ . The process involves irradiating a dilute PPA solution with visible light ( $\lambda > 350\text{ nm}$ ) and monitoring the CD decay of the polymer after a short period of time (40–200 min). Moreover, this irradiation protocol and consequent photochemical electrocyclozation<sup>[78]</sup> of the PPA helix is also useful to identify different helices coexisting in a polymer in solution.

## Results and Discussion

To perform these studies, we selected the PPA that bears the para-ethynylanilide of the (*R*)- $\alpha$ -methoxy- $\alpha$ -trifluoromethylphenylacetic acid (MTPA) [poly-(*R*)-1], because this polymer adopts a *cis-cisoidal* scaffold in non-donor solvents and a *cis-transoidal* one in donor solvents.<sup>[31]</sup> For instance, poly-(*R*)-1 in chloroform, (non-donor/low polar; classification of solvents based on a combination of donor/acceptor properties and polarities together with their dielectric constants and Gutmann's values),<sup>[31]</sup> shows a compressed *cis-cisoidal* polyene scaffold (3 nm helical pitch,  $\omega_1 = 70^\circ$  aprox.), with a *P* orientation of both the internal [positive CD at 377 nm] and the external (AFM) helices (Figure 2a). For its part, when poly-(*R*)-1 is dissolved in THF, (donor/low-polar), the polyene backbone adopts a stretched *cis-transoidal* structure (3.9 nm helical pitch,  $\omega_1$  c.a.  $-155^\circ$ ), where the internal and the external helices are opposite oriented. Thus, while the internal helix has a *M* [CD(-) at 377 nm] helical orientation, the external one rotates in the opposite *P* direction (AFM) (Figure 2b).<sup>[31]</sup> Therefore, from a single polymer, two different structures (*c-c* and *c-t*) can be generated and submitted to photochemical studies.

Thus, two vials containing  $2.1\text{ mg} \cdot 7\text{ mL}^{-1}$  ( $9.00 \cdot 10^{-4}\text{ M}$ ) of poly-(*R*)-1 dissolved in chloroform (vial 1) or in THF (vial 2) under an argon atmosphere were irradiated with visible light ( $\lambda > 350\text{ nm}$ ). 200  $\mu\text{L}$  of these two poly-(*R*)-1 solutions were extracted at different irradiation times and introduced in a 0.1 cm quartz cuvette. ECD studies show that the ECD spectra of the polymer at the vinylic region decreases with time in both solutions, leading to a null CD although at different rates (Figure 2b-c). Adjusting the CD signal decay of the vinyl band—photochemical electrocyclozation process—to a first order reaction showed that the reduction of the 377 nm band to a half height, requires for poly-(*R*)-1 in chloroform, 27 min of irradiation—half-life [ $t_{1/2(377\text{ nm})} = 27\text{ min}$ ], with a rate constant  $K = 2.507 \cdot 10^{-2}\text{ min}^{-1}$  (Figure 2d), while when poly-(*R*)-1 is dissolved in THF the kinetic parameters are  $t_{1/2(377\text{ nm})} = 78\text{ min}$ , and  $K = 8.825 \cdot 10^{-3}\text{ min}^{-1}$  (Figure 2d). GPC monitoring of both experiments shows the disappearance of the well-folded poly-(*R*)-1 chain and its conversion by photochemical electrocyclozation process, which evolve after continuously irradiation with visible light to the corresponding 1,3,5-trisubstituted benzene—1,3,5-(*R*)-1—unambiguously identified by mass spectroscopy (See figures S21 and S22). However, the main goal of this work is not the generation of the 1,3,5-trisubstituted benzene by a photocyclic aromatization process, which has already been described by Aoki and coworkers.<sup>[56]</sup> Herein, we look for the time consumed in the photochemical electrocyclozation process to reach a null ECD signal in the vinylic region, specific for each secondary structure of a PPA. Thus, to study the photochemical electrocyclozation of the polymer, we must monitor the complete disappearance of the polyene ECD band, which is indicative of the loss of its secondary structure. At this stage, no rearomatization with chain cleavage takes place yet and therefore UV-vis studies cannot be used to monitor the photochemical electrocyclozation process, due to the presence of polyenes together with the cyclohexadiene units formed (see Figures S20–S27).

Interestingly, irradiation of samples of poly-(*R*)-1 with different chain lengths produce, at the same concentration and temperature, identical ECD decay patterns, which indicates that the PPA photochemical electrocyclozation process is independent

## RESEARCH ARTICLE

of the polymer size (see Figure S30) being only dependent on the secondary structure of the polymer.

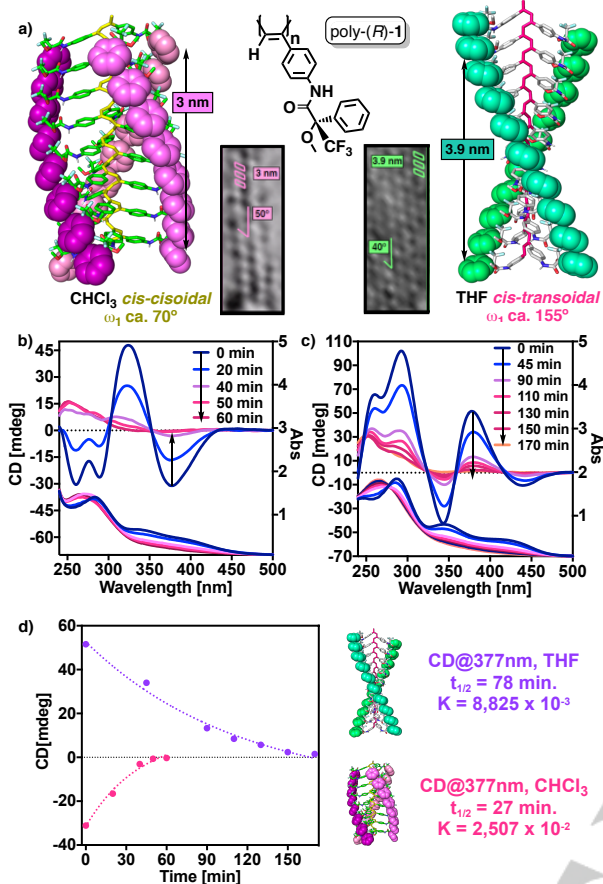


**Figure 2.** (a) 3D structures of poly-(R)-1 in non-donor (CHCl<sub>3</sub>, *cis-cisoidal*) and donor (THF, *cis-transoidal*) solvents. ECD and UV-vis spectra of poly-(R)-1 after irradiation with visible light in (b) CHCl<sub>3</sub> and (c) THF. (d) ECD signal decay vs time for poly-(R)-1 after irradiation with visible light. [poly-(R)-1] =  $9.00 \cdot 10^{-4}$  M (0.3 mg·mL<sup>-1</sup> THF or CHCl<sub>3</sub>). ECD and UV-vis studies were performed in a 0.1 cm quartz cuvette.

Hence, the different kinetic parameters obtained for the photochemical electrocyclization of poly-(R)-1 in CHCl<sub>3</sub> and THF (*c-c* and *c-t* structures respectively) indicate that there is a direct relationship between the helical scaffold—secondary structure—adopted by the polyene skeleton and its sensitivity to light irradiation (Figure 3).

In order to evaluate the scope of this process, the generality of those conclusions, and its potential application as a tool to unequivocally determine the *cis-transoidal* or *cis-cisoidal* scaffold of PPAs, we repeated the visible light irradiation experiments with a series of other PPAs with well-known *c-c* or *c-t* helical structure, as described next.

Poly-(R)-2 bearing the para-ethynylbenzamide of (*R*)-phenylglycine methyl ester as substituent was selected as model compound because adopts a well-known *cis-transoidal* helix (3.8 nm,  $\omega_1$  c.a. 148°) in CHCl<sub>3</sub>,<sup>[43]</sup> with its internal helix *M* oriented [CD(-) at 380 nm], and the external one describing a *P* helix [determined by AFM] (Figure 4a).

Visible light ( $\lambda > 350$  nm) irradiation studies of [poly-(R)-2] dissolved in CHCl<sub>3</sub> (2.1 mg/7·mL,  $1.02 \cdot 10^{-3}$  M) showed a ECD decay that fits to a first order reaction with kinetic parameters:  $t_{1/2}$  (368 nm) = 63 min and  $K = 1.088 \cdot 10^{-2}$  min<sup>-1</sup>— (figure 4b-c).

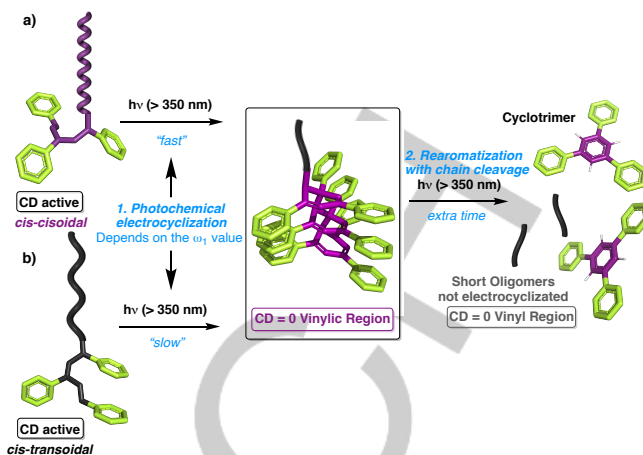


**Figure 3.** Schematic illustration of the two-step photocyclic aromatization reaction—photochemical electrocyclization (formation of cyclohexadiene units in the main chain) + rearomatization with chain cleavage (formation of 1,3,5-trisubstituted benzenes)—in (a) *cis-cisoidal* and (b) *cis-transoidal* polyene scaffolds.

Comparison of the kinetic parameters obtained for poly-(R)-2 and poly-(R)-1 show the values obtained for poly-(R)-2 are similar to those generated for a THF solution of poly-(R)-1, and therefore for a *cis-transoidal* helix (poly-(R)-1  $t_{1/2}$  (THF) = 78 min; poly-(R)-2  $t_{1/2}$  = 63 min), which are clearly different to those obtained when poly-(R)-1 is dissolved in chloroform and corresponds to a *cis-cisoidal* helix (poly-(R)-1  $t_{1/2}$  (CHCl<sub>3</sub>) = 27 min; poly-(R)-2  $t_{1/2}$  = 63 min). Therefore, the photochemical electrocyclization data suggests that poly-(R)-2 in CHCl<sub>3</sub> has a *cis-transoidal* backbone (Figure 4d), needing an extra time for the electrocyclization reaction due to a prior *transoidal* to *cisoidal* photoinduction reaction.

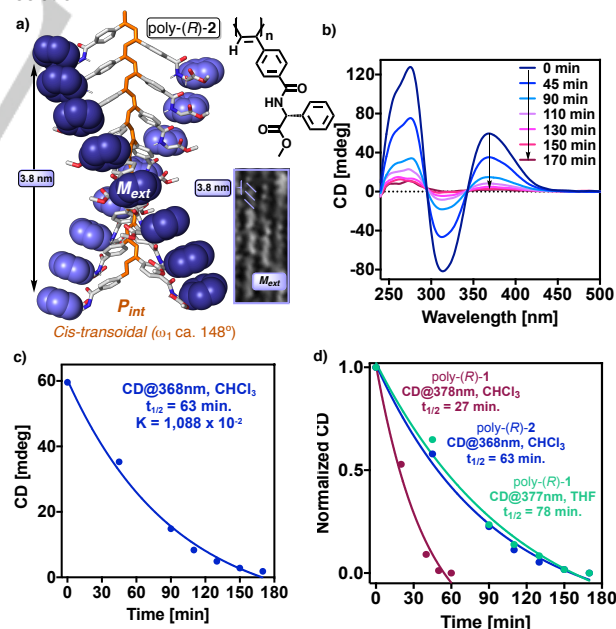


**Figure 4.** (a) Chemical structure and representative helical scaffold adopted by poly-(R)-2. (b) CD spectra of poly-(R)-2 in CHCl<sub>3</sub> at different irradiation times with visible light ( $\lambda > 350$  nm) [poly-(R)-2] =  $1.02 \cdot 10^{-3}$  M. (c) First order reaction fit of the ECD(368 nm) signal decay vs time obtained for the photochemical electrocyclization data suggests that of poly-(R)-2. (d) Comparison of the first order reaction fit obtained for the normalized ECD signal decay vs time corresponding to the photochemical electrocyclization data suggests that of

## RESEARCH ARTICLE

poly-(*R*)-1 in CHCl<sub>3</sub> and THF and poly-(*R*)-2 in CHCl<sub>3</sub>. [poly-(*R*)-1] = 9.00·10<sup>-4</sup> M; [poly-(*R*)-2] = 1.02·10<sup>-3</sup> M. ECD studies were performed in a 0.1 cm quartz cuvette.

These data also indicate that there is a correlation between the elongation of the helix ( $\omega_1$ ) and the time needed for the photochemical electrocyclization data suggests that the one produced before the photocyclic aromatization reaction. Thus, while poly-(*R*)-2 with  $\omega_1$  c.a. 148° needs 63 min for the photochemical electrocyclization, poly-(*R*)-1 with  $\omega_1$  c.a. 155° consumes 15 min. of extra time, due to the presence of a more elongated structure ( $\omega_1$  poly-(*R*)-2 <  $\omega_1$  poly-(*R*)-1).

Another example used to test the correlation between the PPA helical structure and the kinetic parameters of the photochemical electrocyclization process was poly-(*S*)-3, that bears the par-ethynylanilide of (*S*)-mandelic acid as substituent.<sup>[48]</sup> This polymer adopts in CHCl<sub>3</sub> a compressed *cis-cisoidal* helix (3.1 nm,  $\omega_1$  c.a. 70°), where the internal and the external helices are *P* oriented [CD<sub>380nm</sub>(-)] at 368 nm,  $\omega_1$  ca. 70°] (Figure 5a).<sup>[48]</sup>

Irradiation of a chloroform solution of poly-(*S*)-3 (2.1 mg/ 7 mL, 1.19·10<sup>-3</sup> M) showed the expected evolution of the CD signal, which fits to a first order decay—kinetic parameters:  $t_{1/2}$  (386 nm) = 26 min and  $K = 2.68 \cdot 10^{-2} \text{ min}^{-1}$ —(figure 5b-c). In this case, the half-time value obtained for poly-(*S*)-3 is close to the one obtained for a chloroform solution of poly-(*R*)-1 ( $t_{1/2} = 27$  min figure 5d) and coherent with a similar *cis-cisoidal* scaffold ( $\omega_1$  c.a. 70°).

To further explore the  $t_{1/2}/\omega_1$  relationship, we chose as useful example poly-(*S*)-4. This PPA bears the ortho-ethynylanilide of (*S*)- $\alpha$ -methoxy- $\alpha$ -phenylacetic acid as pendant (Figure 6a) and adopts a very stretched -almost flat- helical structure— $\omega_1$  c.a. 170°;  $P_{\text{int}}$  CD<sub>484</sub>(+);  $M_{\text{ext}}$  (AFM)—(Figure 6a).<sup>[49]</sup> Irradiation of poly-(*S*)-4 in CHCl<sub>3</sub> (0.3 mg·mL<sup>-1</sup>, 1.13·10<sup>-3</sup> M) showed a very slow CD<sub>484</sub> signal decay that fits to a first order reaction with a  $t_{1/2}$  (386 nm) = 1513 min and  $K = 4.581 \cdot 10^{-4} \text{ min}^{-1}$ , data that is in full agreement with the presence of an elongated *cis-transoidal* helical structure (Figure 6b-c).

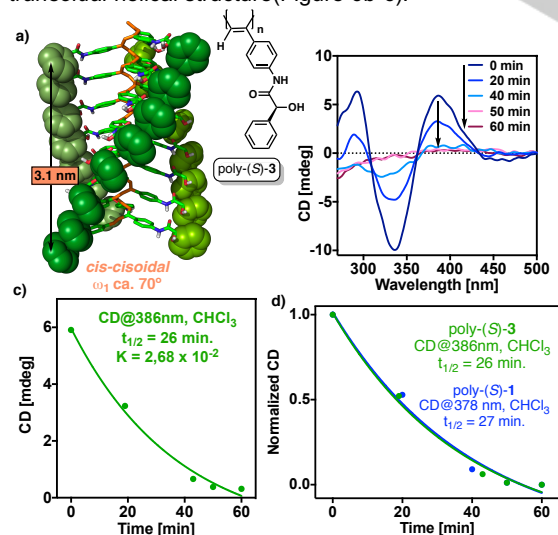


**Figure 5.** (a) Chemical structure and 3D structure of poly-(*S*)-3 in THF (*cis-cisoidal*). (b) ECD spectra of poly-(*S*)-3 after irradiation with visible light in THF. (c) ECD and (d) normalized ECD signal decay vs time for poly-(*S*)-3 after irradiation with visible light. [poly-(*S*)-3] = 1.19·10<sup>-3</sup> M. ECD studies were performed in a 0.1 cm quartz cuvette.

In this case, the photochemical electrocyclization time needed for poly-(*S*)-4 is much higher than those found for other PPAs with *cis-transoidal* skeletons (poly-(*S*)-4  $t_{1/2} = 1513$  min vs. poly-(*R*)-1  $t_{1/2}$  (THF) = 78 min; poly-(*R*)-2  $t_{1/2} = 63$  min). This is due to the presence of a highly stretched almost planar helix (poly-(*S*)-4  $\omega_1$  c.a. 170° vs. poly-(*R*)-1  $\omega_1$  c.a. 155° (THF); poly-(*R*)-2  $\omega_1$  c.a. 148°) and coherent with the structure previously reported (figure 6c).

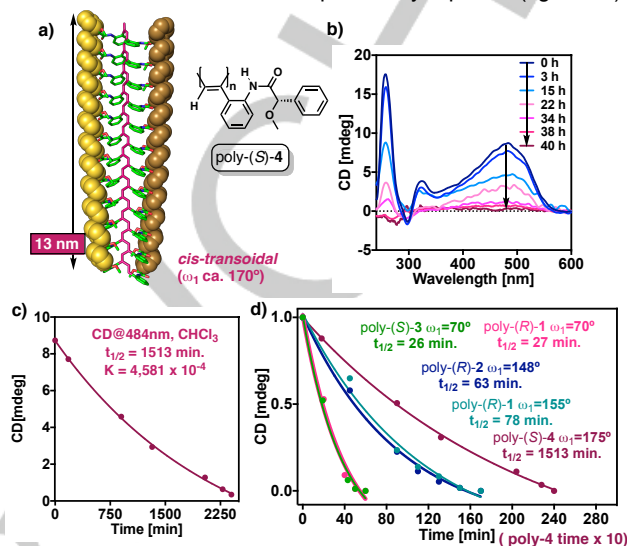


**Figure 6.** (a) Chemical structure and representative *cis-transoidal* helical scaffold adopted by poly-(*S*)-4. (b) CD spectra of poly-(*S*)-4 at different irradiation times under visible light. (c) ECD and (d) normalized ECD signal decay vs time for poly-(*S*)-4 after irradiation with visible light. [poly-(*S*)-4] = 1.13·10<sup>-3</sup> M, CHCl<sub>3</sub>. ECD studies were performed in a 0.1 cm quartz cuvette.

Next, we decided to test the merits of this correlation in more complex systems, namely those PPAs that are constituted by two different scaffolds in equilibrium. Two representative examples are poly-(*S*)-5, that bears the meta-ethynylanilide of (*S*)- $\alpha$ -methoxy- $\alpha$ -phenylacetic acid as substituent and poly-(*R*)-6 with the meta-ethynylbenzamide of (*R*)-phenylglycine methyl ester as pendant.<sup>[49]</sup> Poly-(*S*)-5 in chloroform is constituted by an equilibrium mixture of a compressed *cis-cisoidal*— $\omega_1$  c.a. 70°;  $P_{\text{int}}$  CD<sub>380</sub>(+);  $P_{\text{ext}}$  (AFM)—and a stretched *cis-transoidal*— $\omega_1$  c.a. 155°;  $P_{\text{int}}$  CD<sub>380</sub>(+);  $M_{\text{ext}}$  (AFM)—helices (Figure 7a), while poly-(*R*)-6 in the same solvent is formed by a mixture of two *cis-transoidal* helices with different elongation—helix 1:  $\omega_1$  c.a. 160°,  $P_{\text{int}}$  CD<sub>380</sub>(+),  $M_{\text{ext}}$  (AFM); helix 2:  $\omega_1$  c.a. 165°;  $P_{\text{int}}$  CD<sub>380</sub>(+),  $M_{\text{ext}}$  (AFM)—(Figure 7d).<sup>49</sup> In both cases, poly-(*S*)-5 and poly-(*R*)-6, the polyene band at the CD spectra is constituted by a contribution of the two helical structures, clearly observed in poly-(*R*)-6 by the presence of a CD band with two peaks. Thus, irradiation studies with visible light (520 nm) of chloroform solutions of poly-(*S*)-5 (2.1 mg/ 7 mL; 1.13·10<sup>-3</sup> M) and poly-(*R*)-6 (2.1 mg/ 7 mL; 1.02·10<sup>-3</sup> M) were followed by studying the CD signal decay at two different wavelengths for each polymer, one at the beginning of the Cotton band, and the second at the end—poly-(*S*)-5 CD at 370 and 398 nm; poly-(*R*)-6 CD at 373 and 428 nm). In the case of poly-(*S*)-5, the ECD spectrum obtained in a 0.1 cm quartz cuvette is too weak to analyze the ECD signal decay during the photochemical electrocyclization process. Thus, to improve the ECD signal, a 1 cm quartz cuvette was used to register the ECD spectrum (Figure 7b). The results showed

## RESEARCH ARTICLE

similar kinetic parameters ( $t_{1/2}$ ) for both quartz cuvettes (Figure S35). To corroborate these results, photochemical electrocyclization studies of poly-(*R*)-**6** were carried out in 1 cm and 0.1 cm quartz cuvettes under the same protocols applied to poly-(*S*)-**5**. As expected, the kinetic parameters ( $t_{1/2}$ ) obtained were almost identical (Figure S36).

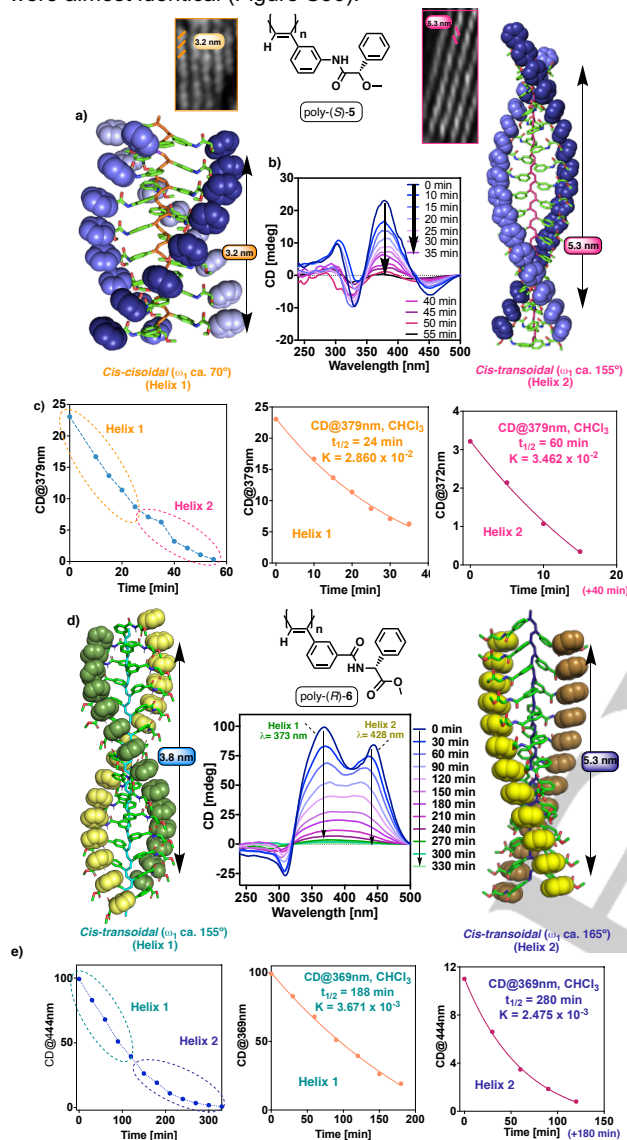


**Figure 7.** (a) Chemical structure and representative *cis-cisoidal* and *cis-transoidal* helical scaffolds adopted by poly-(*S*)-**5**. (b) ECD spectra of poly-(*S*)-**5** at different times of irradiation under visible light. (c) ECD signal decay vs. time for poly-(*S*)-**5** after irradiation with visible light. [poly-(*S*)-**5**] =  $1.13 \cdot 10^{-3}$  M,  $\text{CHCl}_3$ . (d) Chemical structure and representative *cis-transoidal* helical scaffolds adopted by poly-(*R*)-**6** and CD spectra of poly-(*R*)-**6** at different times of irradiation under visible light. (e) ECD signal decay vs. time for poly-(*R*)-**6** after irradiation with visible light. [poly-(*R*)-**6**] =  $1.02 \cdot 10^{-3}$  M,  $\text{CHCl}_3$ . ECD studies were performed in a 1 cm quartz cuvette for poly-(*S*)-**5** and poly-(*R*)-**6**.

The CD signal decay measured at the two wavelengths showed two different slopes for both polymers that correspond to the photochemical electrocyclization processes followed by the existence of two helices in solution (Figure 7 c, e and Figures S35 and S36). For instance, in poly-(*S*)-**5** the photocyclic process takes place between 0 and 60 min for helix 1, while for helix 2 goes from 40 to 90 min. Both curves—helix 1 and helix 2—can

be fitted to a first order reaction, obtaining the following kinetic parameters— $t_{1/2} (379\text{nm}) = 24$  min,  $K = 2.860 \cdot 10^{-2} \text{ min}^{-1}$  for helix 1, and  $t_{1/2} (379\text{nm}) = 60$  min,  $K = 3.462 \cdot 10^{-2} \text{ min}^{-1}$  for helix 2). The data obtained at a different wavelength, 398 nm, provided similar results (Figure S32). Therefore, helix 1 has a half time (25 min) similar to those obtained for poly-(*R*)-**1** (27 min.) and poly-(*S*)-**3** (26 min) that correspond to a *cis-cisoidal* skeleton ( $\omega_1$  c.a.  $70^\circ$ ), while helix 2 has a half time (65 min), close to the one obtained for poly-(*R*)-**2** and that corresponds to a *cis-transoidal* polyene structure ( $\omega_1$  c.a.  $150^\circ$ ).

In the case of poly-(*R*)-**6**, the photochemical electrocyclization of helix 1 takes place between 0 and 180 min, while for helix 2 it goes from 180 to 370 min either at 373 or 428 nm (Figure 7e). Data fitting measured at 373 nm gave the following kinetic parameters— $t_{1/2} (373\text{nm}) = 188$  min,  $K = 3.671 \cdot 10^{-3} \text{ min}^{-1}$  for helix 1, and  $t_{1/2} (373\text{nm}) = 280$  min,  $K = 2.475 \cdot 10^{-3} \text{ min}^{-1}$  for helix 2. Similar data was obtained by fitting the data collected at 428 nm (Figure S26). These results indicate that poly-(*R*)-**6** is composed by two *cis-transoidal* helices, with  $\omega_1$  value in a range of  $150^\circ$ - $170^\circ$ —poly-(*R*)-**1**  $\omega_1$  c.a.  $155^\circ$ ,  $t_{1/2} = 78$  min; poly-(*S*)-**4**  $\omega_1$  c.a.  $170^\circ$ ,  $t_{1/2} = 1513$  min—. The  $\omega_1$  value deduced from these irradiation studies for each helical structure of poly-(*S*)-**5** and poly-(*R*)-**6** are coincident with the information reported in the literature,<sup>[49]</sup> demonstrating again the robustness of the PPA photochemical electrocyclization as structural tool.

Finally, to illustrate the relationship between the  $\omega_1$  and the half-time  $t_{1/2}$  of the photochemical electrocyclization, we plotted the normalized CD signal decay vs. time for all the structures (Figures 8a) and the  $t_{1/2}$  versus their  $\omega_1$  values, taken as a stretching indicator (Figure 8b). This graph not only shows the correlation between  $t_{1/2}$  and  $\omega_1$  values, but also serves to illustrate the dependence of the photochemical electrocyclization process with the *cis-cisoidal* or *cis-transoidal* structure of the original helix, where a *transoidal* to *cisoidal* conformational change is required before the photocyclic reaction to takes place.

This relationship responds to equation (1)

$$Y = Y_0 + (\text{Plateau} - Y_0) \cdot (1 - \exp(-K \cdot x))$$

where  $Y$  is  $\omega_1$ , Plateau is the  $\omega_1$  value at infinite time,  $K$  is the photochemical electrocyclization rate and  $x$  is  $t_{1/2}$ .

Our data were fitted to equation (1), to obtain equation (2) (R square 0.993), useful to determine the approximated  $\omega_1$  from the  $t_{1/2}$ .

$$\omega_1 = -147.5 + 312.6 \cdot (1 - \exp(-4.659 \cdot 10^{-2} \cdot t_{1/2})) \quad (2)$$

As a proof of this concept, we decided to test it with a novel PPA designed to be folded into a compressed (helix 1) and a stretched (helix 2) helix. To this end, we prepared poly-(*R*)-**7** PPA that bears a *meta* substituted (*R*)-MTPA group as pendant— (Figure 9a for synthetic and characterization details).<sup>[97]</sup> Poly-(*R*)-**7** is an isomer of poly-(*R*)-**1**, which has the MTPA group in the *para* position. Next, poly-(*R*)-**7** was submitted to light irradiation in  $\text{CHCl}_3$  and THF ([Poly-(*R*)-**7**] = 2.1 mg/ 7 mL;  $9.00 \cdot 10^{-4}$  M).

Again, the ECD signal obtained for poly-(*R*)-**7** in both solvents was weak when using the 0.1 cm quartz cuvette. Because of this, we present the photochemical electrocyclization studies of this polymer in a 1 cm quartz cuvette (Figure 9) (see Figures S36 and S37 for 0.1 cm quartz cuvette studies).

In both cases, the CD signal showed in coherence with the previous results, the expected decay of the polyene band associated to the photochemical electrocyclization (Figure 7b-c). Plotting the  $\text{CD}_{370}$  signal versus time, in both solvents, gave CD curves with two different slopes corresponding to a mixture of two

## RESEARCH ARTICLE

helices in solution. The following kinetic parameters were obtained after independent first order decay fits of the data in the two solvents.

Poly-(*R*)-7 dissolved in chloroform showed  $t_{1/2}(381\text{nm}) = 32$  min,  $K = 2.131 \cdot 10^{-2} \text{ min}^{-1}$  for helix 1, and  $t_{1/2}(381\text{nm}) = 61$  min,  $K = 4.425 \cdot 10^{-2} \text{ min}^{-1}$  for helix 2. Application of equation 2 to those data gives for helix 1,  $\omega_1 = 89^\circ$ , which corresponds to a *cis-cisoidal* structure and  $\omega_1 = 146^\circ$  for helix 2, that corresponds to a stretched *cis-transoidal* scaffold.

The same study for poly-(*R*)-7 dissolved in THF, afforded  $t_{1/2}(362\text{nm}) = 24$  min,  $K = 2.863 \cdot 10^{-2} \text{ min}^{-1}$  for helix 1, and  $t_{1/2}(362\text{nm}) = 76$  min,  $K = 9.110 \cdot 10^{-3} \text{ min}^{-1}$  for helix 2. These kinetic values correspond to a mixture of a *cis-cisoidal* (helix 1,  $\omega_1 = 60^\circ$ ) and a *cis-transoidal* (helix 2,  $\omega_1 = 156^\circ$ ) helices, in good agreement with the expected  $\omega_1$  value for poly-(*R*)-7.

## CONCLUSIONS

In conclusion, it has been demonstrated through a good number of PPAs with different well-known helical structures—6 polymers, 9 helical scaffolds—that visible light irradiation can be introduced as a powerful technique to determine the secondary structure of polyacetylenes. The basis of the method lies on the quite different rate observed for the photochemical electrocyclization depending on the scaffold (*cis-cisoidal*, *cis-transoidal*) of the helical polymer. To perform these studies, vials containing a dilute solution of a PPA [(poly-(1-6)) = 2.1 mg/ 7 mL; c.a.  $1 \cdot 10^{-3}$  M] was irradiated with visible light ( $\lambda > 350$  nm) and the CD signal decay monitored versus time to afford the photochemical electrocyclization rate and the  $t_{1/2}$  as the relevant parameters.

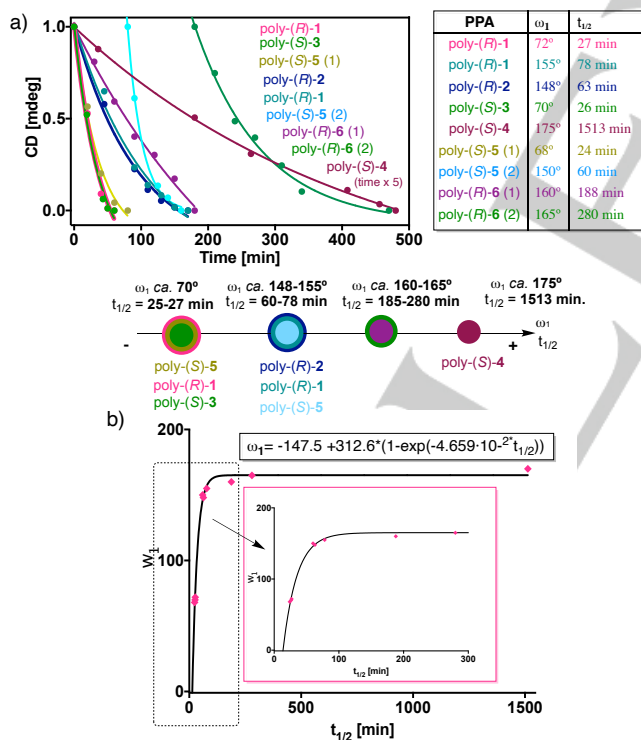


**Figure 8.** a) Normalized CD signal decay of poly(1-6) during photochemical electrocyclization of the different PPA backbones. b) Variation of the PPA  $\omega_1$  vs  $t_{1/2}$  of the backbone photochemical electrocyclization process and the corresponding fit to an exponential equation.

The results show that there is a direct relationship between the elongation of a PPA ( $\omega_1$ ) and its  $t_{1/2}$ . For instance,  $t_{1/2} = 26$  min corresponds to a *cis-cisoidal* PPA with  $\omega_1$  c.a.  $70^\circ$ , such as poly-(*R*)-1 ( $\text{CHCl}_3$ ), poly-(*S*)-3 or poly-(*S*)-5 (helix 1). For their part, PPAs with more elongated chain (larger  $\omega_1$ ) show higher  $t_{1/2}$  values—poly-(*R*)-1 (THF) ( $\omega_1 = 155^\circ$ ,  $t_{1/2} = 78$  min.); poly-(*R*)-2 ( $\omega_1 = 148^\circ$ ,  $t_{1/2} = 63$  min.); poly-(*S*)-4 ( $\omega_1 = 170^\circ$ ,  $t_{1/2} = 1513$  min)—. The kinetic data for all the polymers used in this study, fit well into equation 2 that therefore can be used to predict the scaffold of a PPA ( $\omega_1$ ) from its  $t_{1/2}$  kinetic value. The use of the visible light for the photochemical electrocyclization of PPAs as a tool to determine their helical structure by using a  $t_{1/2}/\omega_1$  relationship, is exceptionally important in this field because no other techniques can provide an approximated value for  $\omega_1$  in solution. This value is necessary to build up an approximated helical structure of the PPA, where important helical parameters such as relative helical sense of the internal and external helices of a PPA depends on this value—*cis-cisoidal* structures ( $\omega_1 < 90^\circ$ ) both helices rotate in the same direction, while in *cis-transoidal* scaffolds ( $\omega_1 > 90^\circ$ ) both helices rotate in opposite directions

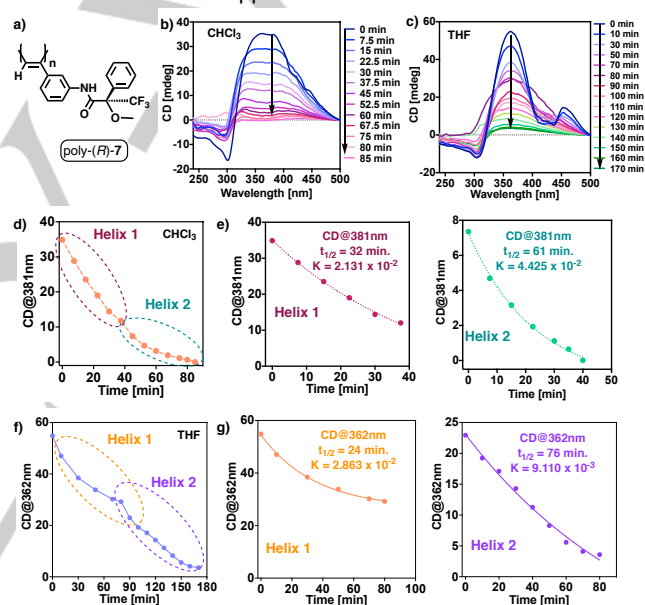


**Figure 9.** (a) Structure of poly-(*R*)-7. (b) CD spectra of poly-(*R*)-7, at different times of irradiation under visible light (c) CD spectra of poly-(*R*)-7, in THF, at different times of irradiation under visible light. (d) ECD signal decay vs time for poly-(*R*)-7 after irradiation with visible light. [poly-(*R*)-7] =  $9.00 \cdot 10^{-4}$  M,  $\text{CHCl}_3$ . (e) ECD signal decay vs time for poly-(*R*)-7 after irradiation with visible light. [poly-(*R*)-7] =  $9.00 \cdot 10^{-4}$  M, THF. (f) Normalized ECD signal decay vs time for poly-(*R*)-7 after irradiation with visible light. ECD studies were performed in a 0.1 cm quartz cuvette.

Although the studies in this work are limited to PPAs substituted by amide groups (anilide, benzamide), no doubt similar investigations can be carried out with other PPAs that bear other connecting groups (ester, ether...). To do this, it will be essential to have a solid base of structural information on these polymers, including AFM images and theoretical calculations, in order to know if the results would be comparable to those of the anilide/benzamide PPAs.

## RESEARCH ARTICLE

## Acknowledgements

Financial support from MINECO (PID2019-109733GB-I00), Xunta de Galicia (ED431C 2018/30, Centro Singular de Investigación de Galicia acreditación 2019-2022, ED431G 2019/03 and F. R. T. and R. R. for predoctoral and postdoctoral fellowships respectively) and the European Regional Development Fund (ERDF) is gratefully acknowledged.

**Keywords:** Photochemistry • Poly(phenylacetylene)s • Helical structure • cis-cisoid • cis-transoid

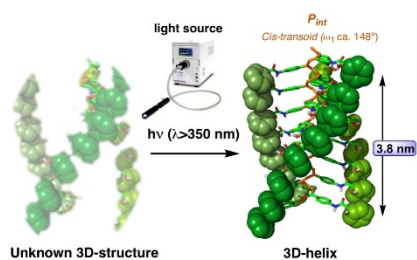
- [1] E. Yashima, N. Ousaka, D. Taura, K. Shimomura, T. Ikai, K. Maeda. *Chem. Rev.*, **2016**, *116*, 13752-13990.
- [2] E. Yashima, K. Maeda, H. Iida, Y. Furusho, K. Nagai. Helical Polymers: Synthesis, Structures, and Functions. *Chem. Rev.*, **2009**, *109*, 6102-6211.
- [3] T. Nakano, Y. Okamoto. Synthetic Helical Polymers: Conformation and Function. *Chem. Rev.*, **2001**, *101*, 4013-4038.
- [4] E. Schwartz, M. Koepf, H. J. Kitto, R. J. M. Nolte, A. E. Rowan. *Polym. Chem.*, **2011**, *2*, 33-47.
- [5] K. Maeda, M. Nozaki, K. Hashimoto, K. Shimomura, D. Hirose, T. Nishimura, G. Watanabe, E. Yashima. *J. Am. Chem. Soc.*, **2020**, *142*, 7668-7682.
- [6] E. Yashima, K. Maeda, Y. Furusho. *Acc. Chem. Res.*, **2008**, *41*, 1166-1180.
- [7] R. Ishidate, A. J. Markvoort, K. Maeda, E. Yashima. *J. Am. Chem. Soc.*, **2019**, *141*, 7605-7614.
- [8] K. Maeda, D. Hirose, N. Okoshi, K. Shimomura, Y. Wada, T. Ikai, S. Kanoh, E. Yashima. *J. Am. Chem. Soc.*, **2018**, *140*, 3270-3276.
- [9] R. Sakai, E. B. Barasa, N. Sakai, S.-I. Sato, T. Satoh, T. Kakuchi. *Macromolecules*, **2012**, *45*, 8221-8227.
- [10] E. Yashima, K. Maeda. *Macromolecules*, **2008**, *41*, 3-12.
- [11] K. Maeda, E. Yashima. *Top. Curr. Chem.* **2006**, *265*, 47-88.
- [12] R. Nonokawa, E. Yashima. *J. Am. Chem. Soc.*, **2003**, *125*, 1278-1283.
- [13] E. Yashima, K. Maeda, Y. Okamoto. *Nature*, **1999**, *399*, 449-451.
- [14] E. Yashima, K. Maeda, T. Matsushima, Y. Okamoto, Y. Chirality, **1997**, *9*, 593-600.
- [15] M. Ando, R. Ishidate, T. Ikai, K. Maeda, E. Yashima. *J. Polym. Sci., Part A: Polym. Chem.* **2019**, *57*, 2481-2490.
- [16] C. Zhang, Y. Qiu, S. Bo, F. Wang, Y. Wang, L. Liu, Y. Zhou, H. Niu, H. Dong, T. Satoh. *J. Polym. Sci., Part A: Polym. Chem.* **2019**, *57*, 1024-1031.
- [17] R. P. Megens, G. Roelfes. *Chem. Eur. J.* **2011**, *17*, 8514-8523.
- [18] E. Anger, H. Iida, T. Yamaguchi, K. Hayashi, D. Kumano, J. Crassous, N. Vanthuyne, C. Roussel, E. Yashima. *Polym. Chem.* **2014**, *5*, 4909-4914.
- [19] R. Ishidate, T. Sato, T. Ikai, S. Kanoh, E. Yashima, K. Maeda. *Polym. Chem.*, **2019**, *10*, 6260-6268.
- [20] D. Hirose, A. Isobe, E. Quiñoá, F. Freire, K. Maeda. *J. Am. Chem. Soc.* **2019**, *141*, 8592-8598.
- [21] J. Shen, Y. Okamoto. *Chem. Rev.*, **2016**, *116*, 1094-1138.
- [22] K. Shimomura, T. Ikai, S. Kanoh, E. Yashima, K. Maeda. *Nat. Chem.* **2014**, *6*, 429-434.
- [23] J. Liu, J. W. Y. Lam, B. Z. Tang. *Chem. Rev.*, **2009**, *109*, 5799-5867.
- [24] C. I. Simionescu, V. Percec. *Prog. Polym. Sci.*, **1982**, *8*, 133-214.
- [25] V. Percec. *Israel J. Chem.* **2020**, *60*, 48-66.
- [26] R. Rodríguez, E. Suárez-Picado, E. Quiñoá, R. Riguera, F. Freire. *Angew. Chem. Int. Ed.* **2020**, *59*, 8616-8622.
- [27] R. Rodríguez, E. Quiñoá, R. Riguera, F. Freire. *Small*, **2019**, *15*, 1805413.
- [28] F. Ishiwari, K. Nakazono, Y. Koyama, T. Takata. *Angew. Chem. Int. Ed.*, **2017**, *56*, 14858-14862.
- [29] R. Rodríguez, S. Arias, E. Quiñoá, R. Riguera, F. Freire. *Nanoscale*, **2017**, *9*, 17752-17757.
- [30] N. Zhu, K. Nakazono, T. Takata. *Chem. Commun.*, **2016**, *52*, 3647-3649.
- [31] S. Leiras, F. Freire, J. M. Seco, E. Quiñoá, R. Riguera. *Chem. Sci.*, **2013**, *4*, 2735-2743.
- [32] K. Maeda, H. Mochizuki, M. Watanabe, E. Yashima. *J. Am. Chem. Soc.*, **2006**, *128*, 7639-7650.
- [33] K. Maeda, N. Kamiya, E. Yashima. *Chem. Eur. J.*, **2004**, *10*, 4000-4010.
- [34] T. Ikai, R. Ishidate, K. Inoue, K. Kaygisiz, K. Maeda, E. Yashima. *Macromolecules*, **2020**, *53*, 973-981.
- [35] M. Alzubi, S. Arias, R. Rodríguez, E. Quiñoá, R. Riguera, F. Freire. *Angew. Chem. Int. Ed.*, **2019**, *58*, 13365-13369.
- [36] R. Rodríguez, E. Quiñoá, R. Riguera, F. Freire. *Chem. Mater.* **2018**, *30*, 2493-2497.
- [37] T. Van Leeuwen, G. H. Heideman, D. Zhao, S. J. Wezenberg, B. L. Feringa. *Chem. Commun.* **2017**, *53*, 6393-6396.
- [38] S. Arias, M. Núñez-Martínez, E. Quiñoá, R. Riguera, F. Freire. *Polym. Chem.*, **2017**, *8*, 3740-3745.
- [39] M. Alzubi, S. Arias, I. Louzao, E. Quiñoá, R. Riguera, F. Freire. *Chem. Commun.*, **2017**, *53*, 8573-8576.
- [40] S. Arias, J. Bergueiro, F. Freire, E. Quiñoá, R. Riguera. *Small*, **2016**, *12*, 238-244.
- [41] S. Arias, F. Freire, E. Quiñoá, R. Riguera. *Polym. Chem.*, **2015**, *6*, 4725-4733.
- [42] F. Freire, J. M. Seco, E. Quiñoá, R. Riguera. *Angew. Chem. Int. Ed.*, **2011**, *50*, 11692-11696.
- [43] I. Louzao, J. M. Seco, E. Quiñoá, R. Riguera. *Angew. Chem. Int. Ed.* **2010**, *49*, 1430-1433.
- [44] V. Percec, E. Aqad, M. Peterca, J. G. Rudick, L. Lemon, J. C. Ronda, B. B. De, P. A. Heiney, E. W. Meijer. *J. Am. Chem. Soc.*, **2006**, *128*, 16365-16372.
- [45] T. Taniguchi, T. Yoshida, K. Echizen, K. Takayama, T. Nishimura, K. Maeda. *Angew. Chem. Int. Ed.* **2020**, *59*, 8670-8680.
- [46] N. S. L. Tan, A. B. Lowe. *Angew. Chem. Int. Ed.*, **2020**, *59*, 5008-5021.
- [47] Z. Ke, S. Abe, T. Ueno, K. Morokuma. *J. Am. Chem. Soc.*, **2011**, *133*, 7926-7941.
- [48] K. Cobos, R. Rodríguez, O. Domarco, B. Fernández, E. Quiñoá, R. Riguera, F. Freire. *Macromolecules*, **2020**, *53*, 3182-3193.
- [49] R. Rodríguez, E. Quiñoá, R. Riguera, F. Freire. *J. Am. Chem. Soc.* **2016**, *138*, 9620-9628.
- [50] Y. Yoshida, Y. Matawari, A. Motoshige, R. Motoshige, T. Hiraoki, M. Wagner, K. Müllen, M. Tabata. *J. Am. Chem. Soc.*, **2013**, *135*, 4110-4116.
- [51] K. Morino, K. Maeda, Y. Okamoto, E. Yashima, T. Sato. *Chem. Eur. J.*, **2002**, *8*, 5112-5120.
- [52] F. Freire, E. Quiñoá, R. Riguera. *Chem. Commun.*, **2017**, *53*, 481-492.
- [53] C. I. Simionescu, V. Percec, S. Dumitrescu. *J. Polym. Sci., Polym. Chem. Ed.* **1977**, *15*, 2497-2509.
- [54] C. I. Simionescu, V. Percec. *J. Polym. Sci. B Polym. Lett. Ed.* **1979**, *17*, 421-429.
- [55] V. Percec. *Polym. Bull.* **1983**, *10*, 1-7.
- [56] L. Liu, T. Namikoshi, Y. Zang, T. Aoki, S. Hadano, Y. Abe, I. Wasuzu, T. Tsutsuba, M. Teraguchi, T. Kaneko. *J. Am. Chem. Soc.*, **2013**, *135*, 602-605.
- [57] H. Shirakawa, T. Ito, S. Ikeda. *Polym. J.* **1973**, *4*, 460-462.
- [58] L. Palomo, R. Rodríguez, S. Medina, E. Quiñoá, J. Casado, F. Freire, F. J. Ramírez. *Angew. Chem. Int. Ed.*, **2020**, *59*, 9080-9087.
- [59] B. Nieto-Ortega, R. Rodríguez, S. Medina, E. Quiñoá, R. Riguera, J. Casado, F. Freire, F. J. Ramírez. *J. Phys. Chem. Lett.*, **2018**, *9*, 2266-2270.
- [60] Tabei, J.; Shiotsuki, M.; Sanda, F.; Masuda, T. *Macromolecules* **2005**, *38*, 9448-9454.
- [61] T. Kaneko, Y. Umeda, T. Yamamoto, M. Tereguchi, T. Aoki. *Macromolecules* **2005**, *38*, 9420-9426.
- [62] F. Takei, H. Hayashi, K. Onitsuka, N. Kobayashi, S. Takahashi. *Angew. Chem. Int. Ed.* **2001**, *40*, 4092-4094.
- [63] R. Rodríguez, J. Ignés-Mullol, F. Sagués, E. Quiñoá, R. Riguera, F. Freire. *Nanoscale*, **2016**, *8*, 3362-3367.
- [64] J. Kumaki. *Polym. J.*, **2016**, *48*, 3-14.
- [65] J. Kumaki, S.-I. Sakurai, E. Yashima. *Chem. Soc. Rev.*, **2009**, *38*, 737-746.
- [66] S.-I. Sakurai, K. Okoshi, J. Kumaki, E. Yashima. *J. Am. Chem. Soc.* **2006**, *128*, 5650-5651.
- [67] K. Okoshi, S.-I. Sakurai, S. Ohsawa, J. Kumaki, E. Yashima. *Angew. Chem. Int. Ed.* **2006**, *45*, 8173-8176.

## RESEARCH ARTICLE

- [68] S.-I. Sakurai, K. Okoshi, J. Kumaki, E. Yashima. *Angew. Chem. Int. Ed.*, **2006**, *45*, 1245-1248.
- [69] V. Percec, J. G. Rudick, M. Peterca, S. R. Staley, M. Wagner, M. Obata, C. M. Mitchell, W.-D. Cho, V. S. K. Balagurusamy, J. N. Lowe, M. Glodde, O. Weichold, K. J. Chung, N. Ghionni, S. N. Magonov, P. A. Heiney. *Chem. Eur. J.*, **2006**, *12*, 5731-5746.
- [70] V. Percec, J. G. Rudick, M. Wagner, M. Obata, C. M. Mitchell, W.-D. Cho, S. N. Magonov. *Macromolecules*, **2006**, *39*, 7342-7351.
- [71] J. G. Rudick and V. Percec. *Macromol. Chem. Phys.*, **2008**, *209*, 1759-1768.
- [72] V. Percec, M. Obata, J. G. Rudick, B. B. De, M. Glodde, T. K. Bera, S. N. Magonov, V. S. K. Balagurusamy, P. A. Heiney. *J. Polym. Sci. Part A Polym. Chem.*, **2002**, *40*, 3509-3533.
- [73] A. Motoshige, Y. Mawatari, R. Motoshige, Y. Yoshida, M. Tabata. *J. Polym. Sci., Part A: Polym. Chem.*, **2013**, *51*, 5177-5183.
- [74] X.-Q. Liu, J. Wang, S. Yang, E.-Q. Chen. *ACS Macro Lett.*, **2014**, *3*, 834-838.
- [75] V. Percec, J. G. Rudick, M. Peterca, E. Aqad, M. R. Imam, P. A. Heiney. *J. Polym. Sci., Part A: Polym. Chem.*, **2007**, *45*, 4974-4987.
- [76] V. Percec, M. Peterca, J. G. Rudick, E. Aqad, M. R. Imam, P. A. Heiney. *Chem.-Eur. J.*, **2007**, *13*, 9572-9581.
- [77] V. Percec, J. G. Rudick, M. Peterca, P. A. Heiney. *J. Am. Chem. Soc.*, **2008**, *130*, 7503-7508.
- [78] V. Percec, J. G. Rudick, M. Peterca, M. Wagner, M. Obata, C. M. Mitchell, W. D. Cho, V. S. K. Balagurusamy, P. A. Heiney. *J. Am. Chem. Soc.*, **2005**, *127*, 15257-15264.
- [79] J. G. Rudick, V. Percec. *Acc. Chem. Res.*, **2008**, *41*, 1641-1652.
- [80] B. L. Feringa, W. R. Browne. *Nature Nanotech.*, **2008**, *3* 383-384.
- [81] A. Miyasaka, T. Sone, Y. Mawatari, S. Setayesh, K. Müllen, M. Tabata. *Macromol. Chem. Phys.*, **2006**, *207*, 1938-1944.
- [82] T. Ito, H. Shirakawa, S. Ikeda. *J. Polym. Sci., Part A: Polym. Chem.*, **1996**, *34*, 2533-2542.
- [83] B. Fernández, R. Rodríguez, E. Quiñoá, R. Riguera, F. Freire. *ACS Omega*, **2019**, *4*, 5233-5240.
- [84] B. Fernández, R. Rodríguez, A. Rizzo, E. Quiñoá, R. Riguera, F. Freire. *Angew. Chem. Int. Ed.*, **2018**, *57*, 3666-3670.
- [85] E. Yashima. *Polymer Journal*, **2010**, *42*, 3-16
- [86] V. Percec, J. G. Rudick, M. Peterca, M. Wagner, M. Obata, C. M. Mitchell, W. D. Cho, V. S. K. Balagurusamy, P. A. Heiney. *J. Am. Chem. Soc.*, **2005**, *127*, 1527-15264.
- [87] J. G. Rudick, V. Percec. *Acc. Chem. Soc.*, **2008**, *41*, 1641-1652.
- [88] B. L. Feringa, W. R. Browne. *Nature Nanotechnology*, **2008**, *3*, 383-383.
- [89] M. Tabata, Y. Tanaka, Y. Sadahiro, T. Sone, K. Yokota, I. Miura. *Macromolecules*, **1997**, *30*, 5200-5204.
- [90] M. Tabata, T. Sone, Y. Sadahiro, K. Yokota. *Macromol. Chem. Phys.*, **1998**, *199*, 1161-1166.
- [91] C. I. Simionescu, V. Percec. *J. Pol. Science: Polymer Chemistry Edition*, **1980**, *18*, 147-155.
- [92] V. Percec, J. G. Rudick. *Macromolecules*, **2005**, *38*, 7241-7250.
- [93] C. I. Simionescu, V. Percec. *J. Pol. Science: Polymer symposia*. **1980**, *67*, 43-71
- [94] V. Percec, J. Rudick, P. Nomber, W. Buchowicz. *J. Polym. Sci., Part A: Polym. Chem.* **2002**, *40*, 3212-3220.
- [95] M. Miyamata, T. Namikoshi, L. Liu, L. Zang, Y. Zang, T. Aoki, Y. Abe, Y. Onimayama, T. Tsubata, M. Teraguchi, T. Kaneko. *Polymer*, **2013**, *54*, 4431-4435.
- [96] L. Liu, G. Zhang, T. Aoki, Y. Wang, T. Kaneko, M. Teraguchi, C. Zhang, H. Dong. *ACS Macro Lett.* **2016**, *5*, 1381-1385.
- [97] Literature show that *meta*-substituted PPAs are usually formed by an equilibrium between a compressed helix, coincident with the one adopted in the *para*-substituted form, and another more elongated one (see references 49 and 50).

## RESEARCH ARTICLE

## Entry for the Table of Contents



The photochemical electrocyclicization of poly(phenylacetylene)s in solution constitutes a novel methodology for obtaining important structural information that allows determine their helical structures —cis-cisoidal ( $\omega_1 < 90^\circ$ ) or cis-transoidal ( $\omega_1 > 90^\circ$ )— while it also provides an estimated value of  $\omega_1$ . In addition, when applied to mixtures, it allows the identification of the different helical scaffolds that coexist in solution.